SCIENCE CHINA
Physics, Mechanics & Astronomy

• Article •

February 2020 Vol. 63 No. 2: 222011
https://doi.org/10.1007/s11433-019-9389-6

# What kind of optical model potentials should be used for deuteron stripping reactions?

XiaoYan Yun[1], DanYang Pang[1,2*], YiPing Xu[1], Zhi Zhang[3], RuiRui Xu[3], ZhongYu Ma[4], and CenXi Yuan[5]

[1]*School of Physics, Beihang University, Beijing 100191, China;*
[2]*Beijing Key Laboratory of Advanced Nuclear Materials and Physics, Beihang University, Beijing 100191, China;*
[3]*China Nuclear Data Center, China Institute of Atomic Energy, Beijing 102413, China;*
[4]*China Institute of Atomic Energy, Beijing 102413, China;*
[5]*Sino-French Institute of Nuclear Engineering and Technology, Sun Yat-Sen University, Zhuhai 519082, China*

Received January 21, 2019; accepted March 8, 2019; published online September 4, 2019

This paper presents the results of a study that compares CTOM, a microscopic optical model potential (OMP), which is an optical model co-created by the China Nuclear Data Center & Tuebingen University, to CH89, which is a typical phenomenological OMP. The respective OMPs were tested by applying them to the modelling of nucleon elastic scattering and $(d, p)$ transfer reactions involving $^{14}$C, $^{36}$S, and $^{58}$Ni targets at both low and relatively high energies. The results demonstrated that although both potentials successfully accounted for the angular distributions of both the elastic scattering and transfer cross sections, the absolute values of the transfer cross sections calculated using CTOM were approximately 25% larger than those calculated using CH89. This increased transfer cross sections allowed CTOM to produce single particle strength reduction factors for the three reactions that were consistent with those extracted from $(e, e'p)$ reactions as well as with more recent $(p, 2p)$ and $(p, pn)$ reactions. Notch tests suggested that nucleon elastic scattering and transfer reactions are sensitive to different regions of the OMP; accordingly, phenomenological OMPs, which are constrained only by elastic scattering cross sections, may not be sufficient for nucleon transfer reactions. Therefore, we suggest that microscopic OMPs, which reflect more theoretical considerations, should be preferred over phenomenological ones in calculations of direct nuclear reactions.

**optical model potentials, elastic scattering, transfer reactions, spectroscopic factors**

**PACS number(s):** 21.10.Pc, 24.50.+g, 25.45.Hi

**Citation:** X.Y. Yun, D. Y. Pang, Y. P. Xu, Z. Zhang, R. R. Xu, Z. Y. Ma and C. X. Yuan, What kind of optical model potentials should be used for deuteron stripping reactions? Sci. China-Phys. Mech. Astron. **63**, 222011 (2020), https://doi.org/10.1007/s11433-019-9389-6

## 1 Introduction

Single nucleon transfer reactions, such as $(d, p)$ and $(p, d)$ reactions, are important tools that are used to study the single particle structure of atomic nuclei, such as spectroscopic factors (SFs) and asymptotic normalization coefficients, which are useful in the study of nuclear shell evolution and nuclear astrophysics [1-12]. In all transfer reaction models, including the distorted wave Born approximation [1], the adiabatic model [13, 14], the Continuum Discretized Coupled-Channel method [5, 15, 16], and Faddeev equation-based models [17-21], microscopic optical model potentials (OMPs) are essential input parameters.

A study of $(d, p)$ and $(p, d)$ reactions by Liu et al. [22] suggested that instead of the OMPs that are fitted to each in-

*Corresponding author (email: dypang@buaa.edu.cn)

 

dividual elastic scattering data, systematic optical model potentials should be used. Use of systematic OMPs reduced the uncertainties of the SFs considerably [22]. There are two kinds of systematic OMPs: phenomenological OMPs, including CH89 and KD02 for nucleons [23,24], OMPs cited in refs. [25-27] for deuterons, GDP08 and A31p [28, 29], OMPs cited in refs. [30-32] for $^3$He and tritons, etc., are obtained by fitting elastic scattering data of a particle within a wide range of incident energies and target masses, and the microscopic OMPs, which originate from more fundamental basis [33-35]. However, due to its complexity, the work of systematic microscopic OMPs is still very rare; phenomenological OMPs are most often used in the analysis of direct nuclear reactions. However, there are two problems in applying phenomenological OMPs to nuclear reactions. First, most of the experimental data from which OMP parameters are determined belong to stable nuclei, and there are considerable uncertainties in extrapolating these potentials to nuclei that are far away from the $\beta$-stability line. Second, it is expected that different types of reactions may be sensitive to different regions of OMPs [36]. Thus, phenomenological OMPs, which are primarily constrained with elastic scattering angular distributions, may not be appropriate to describe other types of reactions, such as nucleon transfer reactions. In this paper, we focus on the second problem.

Recently, CTOM[1)], which is a systematic microscopic optical potential based on the Dirac-Brueckner-Hartree-Fock theory, was proposed by Xu et al. [37, 38]. This potential was found to reasonably reproduce the total and differential cross sections of nucleon elastic scattering from nuclei with masses from $^{12}$C to $^{208}$Pb with incident energies between 100 keV and 250 MeV. In this paper, we examine the application of the CTOM to deuteron stripping reactions and compare the results with those obtained using CH89, which is a typical systematic phenomenological OMP [23]. Three reactions, namely, $^{14}$C$(d,p)^{15}$C, $^{36}$S$(d,p)^{37}$S, and $^{58}$Ni$(d,p)^{59}$Ni are studied at both low and relatively high incident energies, i.e., 14 and 60 MeV, 12.3 and 25 MeV, and 10 and 56 MeV, respectively. We compare CTOM with CH89 for the resulting nucleon elastic scattering and $(d,p)$ transfer reaction cross sections and study their effects on the nuclear structure information extracted from experimental data.

## 2 Model calculations and comparisons

We firstly compare CTOM and CH89 in their resulting nucleon elastic scattering cross sections. A comparison between CH89 and CTOM for the real and imaginary parts of the OMPs of proton with $^{14}$C, $^{36}$S, and $^{58}$Ni is depicted in Figure 1. These OMPs are evaluated at 30, 12.5 and 28 MeV, respectively, which are half values of the corresponding deuteron incident energies. It is observed that the CTOM and CH89 potentials are close in their real parts. Their biggest differences are seen in the imaginary parts: the CTOM potentials are more absorptive than CH89 at radial ranges that are inside the nucleus radius. It is the same for the comparisons of neutron potentials.

It is interesting to note that despite the differences seen in Figure 1, CTOM and CH89 provide rather similar cross sections of nucleon elastic scattering. Figure 2 shows the angular distributions for proton elastic scattering from $^{14}$C, $^{36}$S, and $^{58}$Ni at both low and high energies (7 and 30 MeV, 6.15 and 12.5 MeV, and 5 and 28 MeV, respectively). Both systematic potentials support the same main features of these angular distributions.

We then compared the deuteron stripping cross sections calculated with CTOM and CH89. The reactions were analy-

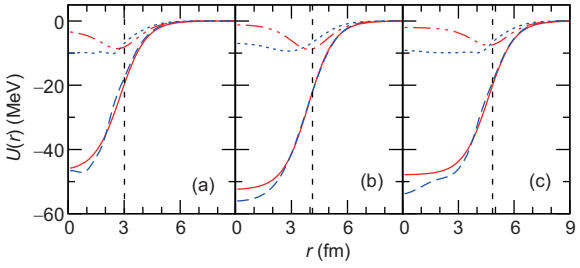


**Figure 1** (Color online) Real and imaginary components of OMPs for proton scattering from (a) $^{14}$C, (b) $^{36}$S, and (c) $^{58}$Ni evaluated at 30, 12.5, and 28 MeV, respectively. The red solid and dashed double-dotted curves represent, respectively, the real and imaginary components of the CH89 potentials; the blue dashed and dotted curves represent the real and imaginary CTOM components, respectively. The vertical dashed lines indicate the root mean square (rms) radii of the target nuclei evaluated as $1.25 \times A_{\rm T}^{1/3}$ with $A$ being the atomic mass numbers of the target nuclei.

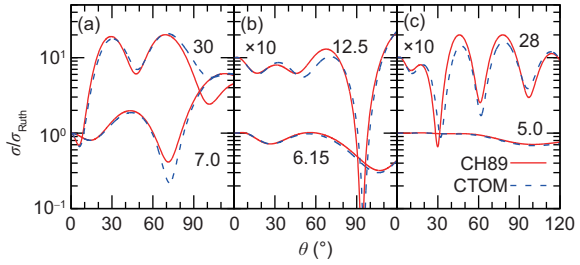


**Figure 2** (Color online) Theoretical predictions of cross sections for proton elastic scattering from (a) $^{14}$C, (b) $^{36}$S, and (c) $^{58}$Ni produced by CH89 (red solid curves) and CTOM (blue dashed curves). The incident energies (MeV) of the protons have been indicated in the figures. Note that some of the cross sections are multiplied by a factor of 10 for optimum visualization.

1) R. R. Xu, Z. Y. Ma, Y. Zhang, Y. Tian, E. N. E. van Dalen, and H. Müther, CTOM: Optical model by cooperation between China Nuclear Data Center and Tuebingen University. http://www.nuclear.csdb.cn/ctom/.

zed using the zero-range adiabatic approximation (ZR-ADWA) [13] with a zero-range normalization factor $D_0 = -125.19$ MeV fm$^{3/2}$. A finite-range correction parameter of $\beta = 0.746$ fm was applied. These parameters are compatible with the deuteron wave function obtained with he Reid-soft-core interaction [39]. All calculations were performed using the computer code TWOFNR[2)]. We note that state-of-the-art theory for deuteron stripping reactions has been proposed in recent years that takes into account the deuteron breakup effects using the CDCC method [4, 8, 16] or by solving the Faddeev equations [17-21]. However, the ADWA remains the most popular reaction model for the analysis of $(d, p)$ and $(p, d)$ reactions [12,40-43]. Since the aim of this work was to study the dependence of OMPs on transfer reactions, we applied ADWA in our analysis. We believe that our conclusions will not change with different reaction models.

In the adiabatic model of a $(d, p)$ reaction, deuteron potential was not needed for the distorted waves of the entrance channel. Instead, an effective deuteron OMP was built using the neutron and proton OMPs evaluated at half of the deuteron incident energies (the "$E_d/2$ rule" [13]). It is worth noting that a previous study of deuteron stripping reactions suggested that, if the nonlocality of the OMPs is taken into account, the effective nucleon incident energies should be shifted by around 40 MeV with respect to the $E_d/2$ rule [44]. We do not believe that the conclusions drawn in this paper will be affected by the nonlocality effects and therefore we retained the $E_d/2$ rule in constructing effective deuteron potentials. However, a study of such effects will be an interesting subject in the future.

In addition to the OMP parameters, the radius and diffuseness parameters of the single particle potentials (in usual Woods-Saxon form) are other important inputs for transfer reactions. Empirical values of these parameters are $r_0 = 1.25$ fm and $a = 0.65$ fm. However, there is no reason for these values to be suitable for each individual nucleus. A better solution should be to confine $r_0$ and $a$ with reliable nuclear structure calculations. In the systematic analysis of nucleon knockout reactions, Gade et al. [45, 46] proposed a procedure with which the $r_0$ and $a$ values are made compatible using the properties of nuclei given by Hartree-Fock (HF) calculations. Subsequently, this procedure was extensively used in the systematic analysis of $(d, p)$ and $(p, d)$ reactions [11, 41]. In this procedure, $a_0$ is fixed to be 0.7 fm and $r_0$ is adjusted so that the mean square radius of the transferred neutron wave function becomes $\langle r^2\rangle = [A/(A-1)]\langle r^2\rangle_{\rm HF}$, where $\langle r^2\rangle_{\rm HF}$ is the value given by HF calculations and $A$ is the mass number of the composite nucleus. This adjustment is carried out using the neutron separation energies given by HF calculations, and the factor $[A/(A-1)]$ is used for correction of fixed potential center assumption used in the HF calculations. These calculations are made for all of the cases studied in this work were using the SkX interaction [47], which is identical to the interactions adopted in the analysis of transfer and knockout reactions in, e.g., refs. [11, 41, 42, 45, 46, 48, 49]. Once $r_0$ and $a_0$ are determined, the depths of the single particle potentials are determined using experimental separation energies.

The resulting $(d, p)$ reaction cross sections calculated using CTOM and CH89 for $^{14}$C, $^{36}$S, and $^{58}$Ni at low and relatively high energies are shown in Figure 3. As in the elastic scattering cases, it is seen that the main features of the angular distributions of transfer cross sections that are calculated using these two systematic OMPs are very close. By matching these theoretical angular distributions to the maxima of the corresponding experimental distributions, the experimental SFs (SF$^{\rm exp}$) of the neutrons in the ground states of the reaction residues were obtained. These SFs are listed in Table 1 together with shell model predictions, SF$^{\rm SM}$. The shell model calculations were performed using YSOX, SDPF-M, and JUN45 interactions [50-52] for $^{15}$C, $^{37}$S, and $^{59}$Ni, respectively. From these results, we obtained the reduction factors, $R_{\rm s}$, of single particle strength for the three nuclei [42]: $R_{\rm s} = {\rm SF}^{\rm exp}/{\rm SF}^{\rm SM}$. The averaged values of the two $R_{\rm s}$ values obtained at the two incident energies are given as $\langle R_{\rm s}\rangle$ in Table 1. The uncertainties in the SF$^{\rm exp}$ and $R_{\rm s}$ values are given as 26%, which include an uncertainty of 20% in the experimental data and input parameters of ADWA calculations [53] as well as an uncertainty of 16% in the choice of reaction models [54].

The quenching of single particle strengths, particularly with respect to dependence on the proton-neutron asymmetry, $\Delta S$, has become a subject of intense debate [42,45,48,55-57], where $\Delta S$ is defined as the difference between the neutron and proton separation energies (i.e., $S_n$ and $S_p$, respectively): for neutron removal $\Delta S = S_n - S_p$ and proton removal $\Delta S = S_p - S_n$. Although systematic analysis of nucleon knockout reactions suggested a strong dependence of the $R_{\rm s}$ values on $\Delta S$ [45,46,48], systematic analysis of $(d, p)$, $(p, d)$, $(p, pn)$, $(p, 2p)$, and $(d,^3{\rm He})$ reactions do not indicate any such dependence [40, 42, 55-57]. The reasons for these systematic discrepancies are currently unknown. However, despite these discrepancies in the dependence on $\Delta S$ values, it is now commonly understood that the single particle strengths should be quenched considerably as compared to the predictions of independent particle or shell models for nuclei that are close to the $\beta$ stability line. Such quenching of single particle strengths is related to some profound problems in

2) J. A. Tostevin. University of surrey version of the code TWOFNR (of M. Toyama, M. Igarashi and N. Kishida) and code front (private communication).

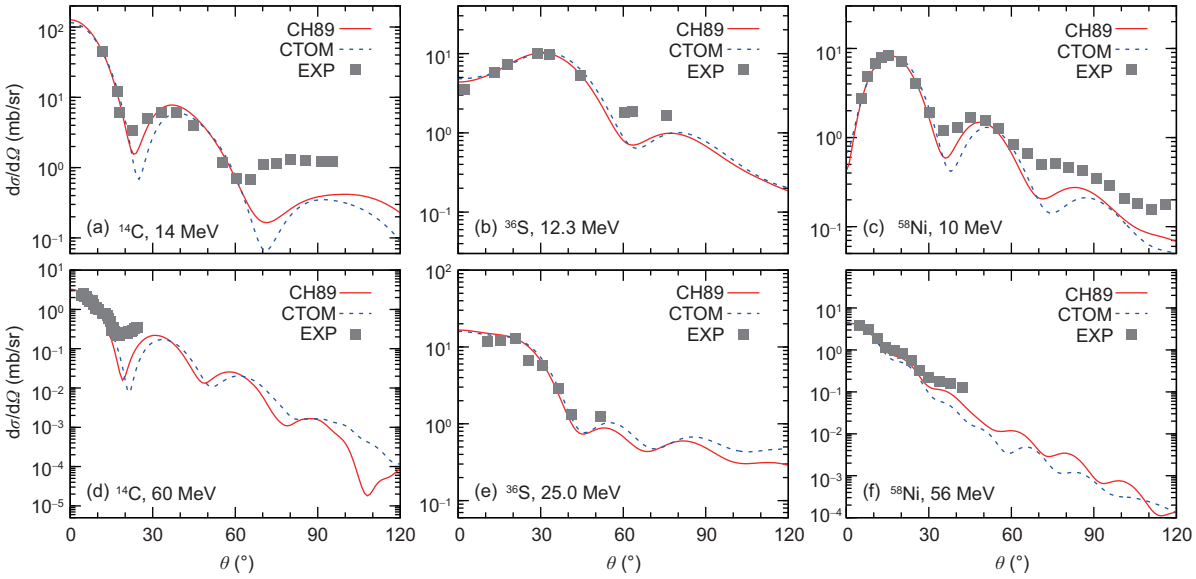


**Figure 3** (Color online) Theoretical (curves) and experimental (symbols) $(d, p)$ reactions with $^{14}$C at (a) 14 MeV and (d) 60 MeV, with $^{36}$S at (b) 12.3 MeV and (e) 25 MeV, and with $^{58}$Ni at (c) 10 MeV and (f) 56 MeV. The theoretical cross sections are normalized to the experimental ones at the maximum cross sections. Calculations made using CH89 and CTOM are indicated by solid and dashed curves, respectively.

**Table 1** Single particle orbitals of transferred neutrons ($nlj$), $r_0$ values of single particle potentials, and incident energies ($E_{\rm lab}$) for the three reactions. The reduction factors of single particle strength ($R_{\rm s}$) are obtained as ratios of experimental and theoretical (shell model) SFs, SF$^{\rm exp}$ and SF$^{\rm SM}$, respectively. $\langle R_{\rm s}\rangle$ are the averaged values of $R_{\rm s}$ evaluated at the two incident energies for each reaction. CH89 and CTOM are analyzed. A unified uncertainty of 26% is applied to the SF$^{\rm exp}$ and $R_{\rm s}$ values. See the text for details

| Target | $nlj$ | $r_0$ (fm) | SF$^{\rm SM}$ | $E_{\rm lab}$ (MeV) | SF$^{\rm exp}$ | $R_{\rm s}$ | $\langle R_{\rm s}\rangle$ | SF$^{\rm exp}$ | $R_{\rm s}$ | $\langle R_{\rm s}\rangle$ |
|---|---|---|---|---|---|---|---|---|---|---|
| | | | | | CH89 | | | CTOM | | |
| $^{14}$C | $2s_{1/2}$ | 1.273 | 1.107 | 14 | 1.11 ± 0.26 | 1.00 ± 0.26 | 0.87 ± 0.23 | 0.75 ± 0.20 | 0.67 ± 0.17 | 0.62 ± 0.16 |
| | | | | 60 | 0.83 ± 0.22 | 0.75 ± 0.20 | | 0.62 ± 0.16 | 0.56 ± 0.15 | |
| $^{36}$S | $1f_{7/2}$ | 1.220 | 0.980 | 12.3 | 0.79 ± 0.21 | 0.81 ± 0.21 | 0.81 ± 0.21 | 0.70 ± 0.18 | 0.72 ± 0.19 | 0.70 ± 0.18 |
| | | | | 25 | 0.79 ± 0.21 | 0.81 ± 0.21 | | 0.67 ± 0.17 | 0.68 ± 0.18 | |
| $^{58}$Ni | $2p_{3/2}$ | 1.154 | 0.572 | 10 | 0.53 ± 0.14 | 0.92 ± 0.24 | 1.04 ± 0.27 | 0.38 ± 0.10 | 0.66 ± 0.17 | 0.69 ± 0.18 |
| | | | | 56 | 0.66 ± 0.17 | 1.15 ± 0.30 | | 0.41 ± 0.11 | 0.72 ± 0.19 | |

nuclear physics, such as short- and medium-range nucleon-nucleon correlations, long-range correlations arising from the coupling of the single particle motions of nucleons near the Fermi surface, and the collective excitations [58-60].

The results in Figures 2 and 3 show that CTOM and CH89 provide very similar angular distributions for both elastic and transfer reactions. However, as seen from Table 1, the absolute values of the transfer cross sections calculated using CTOM are approximately 25% larger than those calculated using CH89, which can be observed from the average value of the ratios between the SF$^{\rm exp}$ values extracted by the respective OMPs. This discrepancy may be linked to the fact that elastic scattering cross sections are solely determined by the asymptotics while transfer amplitudes involve the integrals of the distorted waves. The fact that the two systematic OMPs provide similar elastic scattering angular distributions but different transfer reaction amplitudes may indicate that the distorted waves with these OMPs are similar outside of the range of the OMPs but are different internally. These discrepancies, in turn, might relate to difference in the regions of radial sensitivity of elastic scattering and transfer reactions, which can be examined using a notch test [61-63].

Details of the notch test protocol can be found in ref. [63]; here, we only briefly describe its application in this study. An OMP with a notch at radius $R_{\rm no}$ is as follows:

$$U'(r) = U(r) \times \left[1 - N_{\rm no} {\rm e}^{-[(r-R_{\rm no})/a_{\rm no}]^2}\right], \quad (1)$$

where $U(r)$ is the unperturbed potential and $N_{\rm no}$ and $a_{\rm no}$ are the amplitude and range of the notch (perturbation), respectively, which here are set to $N_{\rm no} = 0.3$ and $a_{\rm no} = 0.5$ fm, respectively. As an example, we show in Figure 4 the real and imaginary parts of $U'$ with notches at 1, 3, 5, and 7 fm along with the unperturbed potential for comparison.

The effect on the elastic scattering and transfer cross sec-

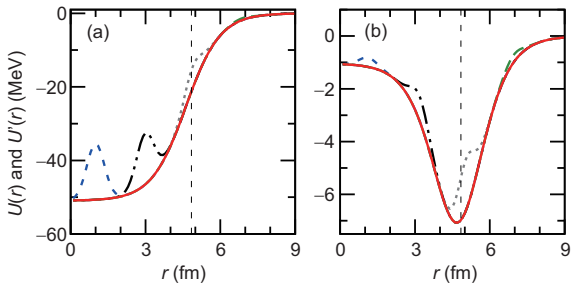


**Figure 4** (Color online) Curves showing (a) real and (b) imaginary components of unperturbed and perturbed OMPs for $n$+$^{58}$Ni at 5 MeV. Perturbed OMPs with notches at $R_{\rm no}$ = 1, 3, 5, and 7 fm are indicated by dashed, dash-double-dotted, dotted, and long dashed curves, respectively. The unperturbed potential (solid) is evaluated using CH89 systematics. The vertical dashed lines indicate the rms radius of the target nucleus evaluated at $1.25 \times 58^{1/3}$.

tions of the notches in the OMPs can be quantified in terms of the standard $\chi^2$ values, which depend on the notch radius $R_{\rm no}$ and can be given as follows:

$$\chi^2(R_{\rm no}) = \frac{1}{N}\sum_i^N \frac{(\sigma_i - \sigma_i^{\rm no})^2}{(\Delta\sigma_i)^2}, \tag{2}$$

where, $\sigma_i$ and $\sigma_i^{\rm no}$ are the cross sections obtained under the unperturbed and perturbed potentials, respectively, that are evaluated with the center-of-mass scattering angle $\theta_i$ summed from 1 to 120 degrees in 1 degree steps. We assume that the cross sections have a uniform uncertainty of 15% $\Delta\sigma_i = 0.15 \times \sigma_i$.

The results of notch tests for elastic scattering and transfer reactions corresponding to the low and higher energies are shown in Figure 5, in which, the top and bottom panels are for notches on the real and imaginary parts of the OMPs, respectively. This notch is made with respect to the CH89 potentials. This notch is made with respect to the CH89 potentials for both the effective deuteron and proton-target potentials in the entrance and the exit channels. The results based on the CTOM are similar and are not shown for clarity. Note that all the $\chi^2$ values are normalized so that their maximum values are unity.

One immediate impression obtained from Figure 5 is that both elastic scattering and transfer cross sections are sensitive to the internal part of the real potentials and to the external part of the imaginary potentials. This is in accordance with results obtained for proton elastic scattering from $^{12}$C reported in ref. [61] and alpha particle scattering from $^{44}$Ti [62]. This may relate to the fact that the imaginary potentials represent the absorption of incident particles, which mainly occurs at the surfaces of the target nuclei. More importantly, it is observed that the radial sensitive regions in the OMPs for the elastic scattering and transfer cross sections are quite different. For instance, for the $^{14}$C$(d, p)^{15}$C reaction at 30 MeV/nucleon, transfer reaction is more sensitive to the internal part of the OMP than elastic scattering does, for both the real and imaginary parts. At 7 MeV/nucleon incident energies, however, the elastic scattering cross sections are sensitive to the real potential within a range that is considerably larger than that in which the transfer reaction is sensitive, although the maximum $\chi^2$ values appear in different regions: externally for the elastic scattering and internally for the transfer cross sections. Conversely, the region in which the elastic scattering is sensitive to is more localized in the imaginary component and its maximum $\chi^2$ value appears more internally than that of the transfer reaction, although both are outside the radius of $^{14}$C. The comparisons between the sensitive regions of elastic scattering and transfer reactions for the other two reactions differ from those occurring in the $^{14}$C$(d, p)^{15}$C reaction. Especially, many oscillations appear in the $^{58}$Ni real potentials under notch testing, which suggests stronger interference between the internal and external components of the transfer amplitudes for this reaction [6].

Overall, however, we see no cases in which elastic scattering and transfer reactions are sensitive to the same regions in both the real and imaginary components of the optical potentials. From this we can conclude that phenomenological OMPs, normally constrained by elastic scattering angular distribution only, could not, in general, represent interactions between projectile and target nuclei appropriately in all regions that are important for transfer reactions. This suggests that microscopic OMPs, which are based on more fundamental principles of nuclear many body interactions, might be more appropriate for the purposes of describing elastic scattering and transfer reactions simultaneously and for reliably extracting nuclear structure information. In fact, it is seen from Table 1 that the averaged $R_{\rm s}$ values obtained under CTOM are all within the range 0.6-0.7, which is in close agreement with the values obtained in ref. [41] for $(d, p)$ and $(p, p)$ reactions and in the most recent analysis of $(p, 2p)$, $(p, pn)$ reactions [55-57]. Conversely, the $R_{\rm s}$ values obtained with CH89 are systematically larger. We have checked that the use of the other popular phenomenological OMP, KD02 [24], results in nearly the same $R_{\rm s}$ values as those produced by CH89. We note that the reduction of the single particle strengths relative to those obtained from the systematic analysis of $(e, e'p)$ reactions, which are free from the uncertainties of OMPs and are thus deemed to be more reliable, lie within the range between 0.4 and 0.7 approximately [64]. The fact that the $R_{\rm s}$ values obtained under microscopic OMP (CTOM) agree with the systematics of $(e, e'p)$ reactions more closely than those obtained with phenomenologically OMP (CH89) suggests that microscopic OMPs can produce more reliable nu-

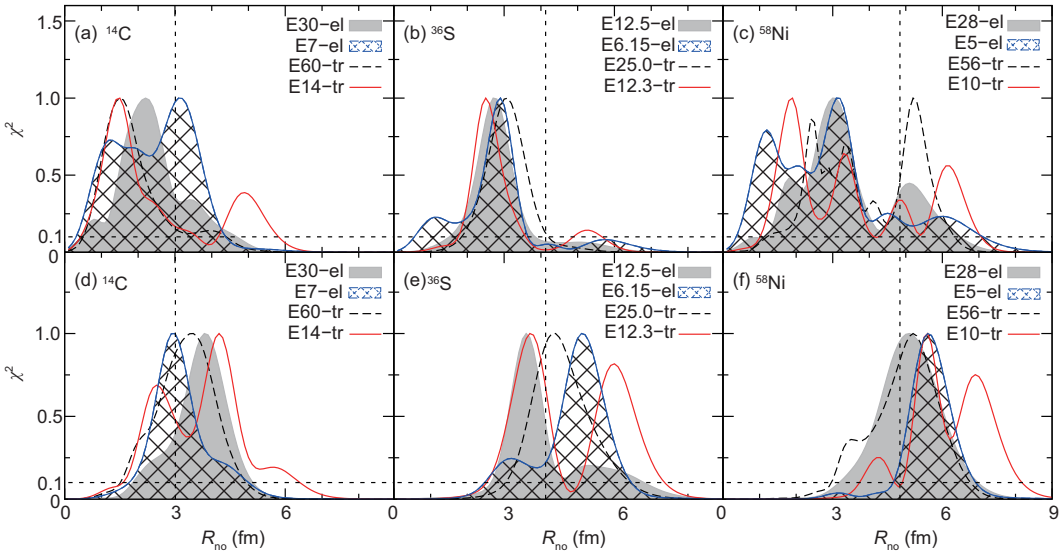


**Figure 5** (Color online) Normalized $\chi^2$ values as functions of the notch radius $R_{no}$ for proton elastic scattering (areas labeled with "el") and $(d, p)$ reactions (curves labeled with "tr") on $^{14}$C ((a) and (d)), $^{36}$S ((b) and (e)), and $^{58}$Ni ((c) and (f)) targets. Incident energies of protons and deuterons are indicated as the numbers after "E". The grid areas and solid curves correspond to the low energy cases, and the shaded areas and dashed curves correspond to relatively higher energies. The top and bottom panels correspond to notches on the real and imaginary potentials, respectively. The vertical dashed lines indicate the rms radii of the target nuclei.

clear structure information, and therefore, should be used in the analysis of $(d, p)$ and $(p, d)$ reactions. It would be interesting to see if the testing of other microscopic OMPs leads to the same conclusion.

## 3 Summary

Optical model potentials are important inputs in direct nuclear reaction calculations. In this study, we compare the application of the microscopic OMP, CTOM, and the phenomenological OMP, CH89, in nucleon elastic scattering and transfer reactions with $^{14}$C, $^{36}$S and $^{58}$Ni at both low and relatively higher energies. Our results show that both systematic potentials account well for the angular distributions of both the elastic scattering and transfer cross sections. However, the amplitudes of the transfer cross sections with CTOM are about 25% larger than those with CH89. As a result, the reduction factors of the single particle strengths extracted from these three reactions are decreased with CTOM and fall within the range of the systematics of the $(e, e'p)$ reactions. The results of notch test suggest that nucleon elastic scattering and transfer reactions are sensitive to different regions of the optical model potentials, which in turn suggests that phenomenological OMPs, which are primarily constrained with elastic scattering cross section, might not be sufficient for nucleon transfer reactions. This may also be the reason for the fact that the CTOM, which is based on more fundamental principles of nuclear interactions, allowed us to get more reliable nuclear structure information than CH89 does. From these results we conclude that microscopic OMPs should be preferred instead of phenomenological OMPs in direct nuclear reactions.

*This work was supported by the National Natural Science Foundation of China (Grant Nos. 11775013, U1432247, 11775316, U1630143, and 11465005), the National Key Research and Development Program (Grant No. 2016YFA0400502), and Science Challenge Project (Grant No. TZ2018001).*

1 N. Austern, *Direct Nuclear Reaction Theories* (Academic, New York, 1970).
2 D. Y. Pang, F. M. Nunes, and A. M. Mukhamedzhanov, Phys. Rev. C **75**, 024601 (2007).
3 Z. H. Li, J. Su, B. Guo, Z. C. Li, X. X. Bai, J. C. Liu, Y. J. Li, S. Q. Yan, B. X. Wang, Y. B. Wang, G. Lian, S. Zeng, E. T. Li, Y. S. Chen, N. C. Shu, Q. W. Fan, and W. P. Liu, Sci. China-Phys. Mech. Astron. **53**, 658 (2010).
4 D. Y. Pang, N. K. Timofeyuk, R. C. Johnson, and J. A. Tostevin, Phys. Rev. C **87**, 064613 (2013), arXiv: 1306.2706.
5 D. Y. Pang, and A. M. Mukhamedzhanov, Phys. Rev. C **90**, 044611 (2014).
6 A. M. Mukhamedzhanov, D. Y. Pang, C. A. Bertulani, and A. S. Kadyrov, Phys. Rev. C **90**, 034604 (2014), arXiv: 1408.5641.
7 X. C. Du, B. Guo, Z. H. Li, D. Y. Pang, E. T. Li, and W. P. Liu, Sci. China-Phys. Mech. Astron. **58**, 062001 (2015).
8 A. M. Mukhamedzhanov, and D. Y. Pang, Phys. Rev. C **92**, 014625 (2015).
9 W. Jiang, Y. L. Ye, Z. H. Li, C. J. Lin, Q. T. Li, Y. C. Ge, J. L. Lou, D. X. Jiang, J. Li, Z. Y. Tian, J. Feng, B. Yang, Z. H. Yang, J. Chen, H. L. Zang, Q. Liu, P. J. Li, Z. Q. Chen, Y. Zhang, Y. Liu, X. H. Sun, J. Ma, H. M. Jia, X. X. Xu, L. Yang, N. R. Ma, and L. J. Sun, Sci. China-Phys. Mech. Astron. **60**, 062011 (2017).
10 Z. H. Li, Y. J. Li, J. Su, S. Q. Yan, Y. B. Wang, B. Guo, D. Nan, E. T. Li, L. Gan, and W. P. Liu, Sci. China-Phys. Mech. Astron. **62**, 032021 (2019).
11 Y. P. Xu, D. Y. Pang, X. Y. Yun, S. Kubono, C. A. Bertulani, and C. X. Yuan, Phys. Rev. C **98**, 044622 (2018), arXiv: 1809.04204.

12 J. Chen, J. L. Lou, Y. L. Ye, Z. H. Li, D. Y. Pang, C. X. Yuan, Y. C. Ge, Q. T. Li, H. Hua, D. X. Jiang, X. F. Yang, F. R. Xu, J. C. Pei, J. Li, W. Jiang, Y. L. Sun, H. L. Zang, Y. Zhang, G. Li, N. Aoi, E. Ideguchi, H. J. Ong, J. Lee, J. Wu, H. N. Liu, C. Wen, Y. Ayyad, K. Hatanaka, D. T. Tran, T. Yamamoto, M. Tanaka, and T. Suzuki, Phys. Rev. C **98**, 014616 (2018).
13 R. C. Johnson, and P. J. R. Soper, Phys. Rev. C **1**, 976 (1970).
14 R. C. Johnson, and P. C. Tandy, Nucl. Phys. A **235**, 56 (1974).
15 D. Y. Pang, and R. S. Mackintosh, Phys. Rev. C **84**, 064611 (2011).
16 H. J. Ong, I. Tanihata, A. Tamii, T. Myo, K. Ogata, M. Fukuda, K. Hirota, K. Ikeda, D. Ishikawa, T. Kawabata, H. Matsubara, K. Matsuta, M. Mihara, T. Naito, D. Nishimura, Y. Ogawa, H. Okamura, A. Ozawa, D. Y. Pang, H. Sakaguchi, K. Sekiguchi, T. Suzuki, M. Taniguchi, M. Takashina, H. Toki, Y. Yasuda, M. Yosoi, and J. Zenihiro, Phys. Lett. B **725**, 277 (2013), arXiv: 1205.4296.
17 E. O. Alt, L. D. Blokhintsev, A. M. Mukhamedzhanov, and A. I. Sattarov, Phys. Rev. C **75**, 054003 (2007).
18 A. Deltuva, Phys. Rev. C **88**, 011601 (2013).
19 A. Deltuva, Phys. Rev. C **91**, 024607 (2015), arXiv: 1502.04913.
20 A. Deltuva, A. Ross, E. Norvaišas, and F. M. Nunes, Phys. Rev. C **94**, 044613 (2016), arXiv: 1610.04448.
21 A. Deltuva, D. Jurčiukonis, and E. Norvaišas, Phys. Lett. B **769**, 202 (2017), arXiv: 1703.09289.
22 X. D. Liu, M. A. Famiano, W. G. Lynch, M. B. Tsang, and J. A. Tostevin, Phys. Rev. C **69**, 064313 (2004).
23 R. L. Varner, W. J. Thompson, T. L. McAbee, E. J. Ludwig, and T. B. Clegg, Phys. Rep. **201**, 57 (1991).
24 A. J. Koning, and J. P. Delaroche, Nucl. Phys. A **713**, 231 (2003).
25 W. W. Daehnick, J. D. Childs, and Z. Vrcelj, Phys. Rev. C **21**, 2253 (1980).
26 H. An, and C. Cai, Phys. Rev. C **73**, 054605 (2006).
27 Y. Han, Y. Shi, and Q. Shen, Phys. Rev. C **74**, 044615 (2006).
28 D. Y. Pang, P. Roussel-Chomaz, H. Savajols, R. L. Varner, and R. Wolski, Phys. Rev. C **79**, 024615 (2009).
29 D. Y. Pang, W. M. Dean, and A. M. Mukhamedzhanov, Phys. Rev. C **91**, 024611 (2015).
30 X. Li, C. Liang, and C. Cai, Nucl. Phys. A **789**, 103 (2007).
31 H. Guo, Y. Zhang, Y. Han, and Q. Shen, Phys. Rev. C **79**, 064601 (2009).
32 C. T. Liang, X. H. Li, and C. H. Cai, J. Phys. G-Nucl. Part. Phys. **36**, 085104 (2009).
33 J. P. Jeukenne, A. Lejeune, and C. Mahaux, Phys. Rev. C **16**, 80 (1977).
34 D. Bonatsos, and H. Müther, Nucl. Phys. A **510**, 55 (1990).
35 B. Q. Chen, and A. D. MacKellar, Phys. Rev. C **52**, 878 (1995).
36 J. G. Camacho, and A. M. Moro, *A Pedestrian Approach to the Theory of Transfer Reactions: Application to Weakly-Bound and Unbound Exotic Nuclei* (Berlin, Heidelberg, 2014), pp. 39-66.
37 R. Xu, Z. Ma, E. N. E. van Dalen, and H. Müther, Phys. Rev. C **85**, 034613 (2012), arXiv: 1203.3355.
38 R. Xu, Z. Ma, Y. Zhang, Y. Tian, E. N. E. van Dalen, and H. Müther, Phys. Rev. C **94**, 034606 (2016), arXiv: 1605.07778.
39 L. D. Knutson, J. A. Thomson, and H. O. Meyer, Nucl. Phys. A **241**, 36 (1975).
40 M. B. Tsang, J. Lee, and W. G. Lynch, Phys. Rev. Lett. **95**, 222501 (2005).
41 J. Lee, J. A. Tostevin, B. A. Brown, F. Delaunay, W. G. Lynch, M. J. Saelim, and M. B. Tsang, Phys. Rev. C **73**, 044608 (2006).
42 J. Lee, M. B. Tsang, D. Bazin, D. Coupland, V. Henzl, D. Henzlova, M. Kilburn, W. G. Lynch, A. M. Rogers, A. Sanetullaev, A. Signoracci, Z. Y. Sun, M. Youngs, K. Y. Chae, R. J. Charity, H. K. Cheung, M. Famiano, S. Hudan, P. OMalley, W. A. Peters, K. Schmitt, D. Shapira, and L. G. Sobotka, Phys. Rev. Lett. **104**, 112701 (2010), arXiv: 0911.4857.
43 J. Chen, J. L. Lou, Y. L. Ye, Z. H. Li, D. Y. Pang, C. X. Yuan, Y. C. Ge, Q. T. Li, H. Hua, D. X. Jiang, X. F. Yang, F. R. Xu, J. C. Pei, J. Li, W. Jiang, Y. L. Sun, H. L. Zang, Y. Zhang, N. Aoi, E. Ideguchi, H. J. Ong, J. Lee, J. Wu, H. N. Liu, C. Wen, Y. Ayyad, K. Hatanaka, D. T. Tran, T. Yamamoto, M. Tanaka, and T. Suzuki, Phys. Lett. B **781**, 412 (2018), arXiv: 1805.06074.
44 N. K. Timofeyuk, and R. C. Johnson, Phys. Rev. Lett. **110**, 112501 (2013).
45 A. Gade, P. Adrich, D. Bazin, M. D. Bowen, B. A. Brown, C. M. Campbell, J. M. Cook, T. Glasmacher, P. G. Hansen, K. Hosier, S. McDaniel, D. McGlinchery, A. Obertelli, K. Siwek, L. A. Riley, J. A. Tostevin, and D. Weisshaar, Phys. Rev. C **77**, 044306 (2008).
46 J. A. Tostevin, and A. Gade, Phys. Rev. C **90**, 057602 (2014), arXiv: 1409.6576.
47 B. Alex Brown, Phys. Rev. C **58**, 220 (1998).
48 A. Gade, D. Bazin, B. A. Brown, C. M. Campbell, J. A. Church, D. C. Dinca, J. Enders, T. Glasmacher, P. G. Hansen, Z. Hu, K. W. Kemper, W. F. Mueller, H. Olliver, B. C. Perry, L. A. Riley, B. T. Roeder, B. M. Sherrill, J. R. Terry, J. A. Tostevin, and K. L. Yurkewicz, Phys. Rev. Lett. **93**, 042501 (2004).
49 C. Wen, Y. P. Xu, D. Y. Pang, and Y. L. Ye, Chin. Phys. C **41**, 054104 (2017).
50 C. Yuan, T. Suzuki, T. Otsuka, F. Xu, and N. Tsunoda, Phys. Rev. C **85**, 064324 (2012), arXiv: 1209.5587.
51 Y. Utsuno, T. Otsuka, T. Mizusaki, and M. Honma, Phys. Rev. C **60**, 054315 (1999).
52 M. Honma, T. Otsuka, T. Mizusaki, and M. Hjorth-Jensen, Phys. Rev. C **80**, 064323 (2009).
53 J. Lee, M. B. Tsang, and W. G. Lynch, arXiv: nucl-ex/0511024.
54 F. M. Nunes, and A. Deltuva, Phys. Rev. C **84**, 034607 (2011), arXiv: 1108.2519.
55 M. Gómez-Ramos, and A. M. Moro, Phys. Lett. B **785**, 511 (2018), arXiv: 1808.09342.
56 L. Atar, S. Paschalis, C. Barbieri, C. A. Bertulani, P. Díaz Fernández, M. Holl, M. A. Najafi, V. Panin, H. Alvarez-Pol, T. Aumann, V. Avdeichikov, S. Beceiro-Novo, D. Bemmerer, J. Benlliure, J. M. Boillos, K. Boretzky, M. J. G. Borge, M. Caamaño, C. Caesar, E. Casarejos, W. Catford, J. Cederkall, M. Chartier, L. Chulkov, D. Cortina-Gil, E. Cravo, R. Crespo, I. Dillmann, Z. Elekes, J. Enders, O. Ershova, A. Estrade, F. Farinon, L. M. Fraile, M. Freer, D. Galaviz Redondo, H. Geissel, R. Gernhäuser, P. Golubev, K. Göbel, J. Hagdahl, T. Heftrich, M. Heil, M. Heine, A. Heinz, A. Henriques, A. Hufnagel, A. Ignatov, H. T. Johansson, B. Jonson, J. Kahlbow, N. Kalantar-Nayestanaki, R. Kanungo, A. Kelic-Heil, A. Knyazev, T. Kröll, N. Kurz, M. Labiche, C. Langer, T. Le Bleis, R. Lemmon, S. Lindberg, J. Machado, J. Marganiec-Gałązka, A. Movsesyan, E. Nacher, E. Y. Nikolskii, T. Nilsson, C. Nociforo, A. Perea, M. Petri, S. Pietri, R. Plag, R. Reifarth, G. Ribeiro, C. Rigollet, D. M. Rossi, M. Röder, D. Savran, H. Scheit, H. Simon, O. Sorlin, I. Syndikus, J. T. Taylor, O. Tengblad, R. Thies, Y. Togano, M. Vandebrouck, P. Velho, V. Volkov, A. Wagner, F. Wamers, H. Weick, C. Wheldon, G. L. Wilson, J. S. Winfield, P. Woods, D. Yakorev, M. Zhukov, A. Zilges, and K. Zuber, Phys. Rev. Lett. **120**, 052501 (2018).
57 S. Kawase, T. Uesaka, T. L. Tang, D. Beaumel, M. Dozono, T. Fukunaga, T. Fujii, N. Fukuda, A. Galindo-Uribarri, S. Hwang, N. Inabe, T. Kawabata, T. Kawahara, W. Kim, K. Kisamori, M. Kobayashi, T. Kubo, Y. Kubota, K. Kusaka, C. Lee, Y. Maeda, H. Matsubara, S. Michimasa, H. Miya, T. Noro, Y. Nozawa, A. Obertelli, K. Ogata, S. Ota, E. Padilla-Rodal, S. Sakaguchi, H. Sakai, M. Sasano, S. Shimoura, S. Stepanyan, H. Suzuki, T. Suzuki, M. Takaki, H. Takeda, A. Tamii, H. Tokieda, T. Wakasa, T. Wakui, K. Yako, J. Yasuda, Y. Yanagisawa, R. Yokoyama, K. Yoshida, K. Yoshida, and J. Zenihiro, Prog. Theor. Exp. Phys. **2018(2)**, 021D01 (2018).
58 J. W. A. den Herder, H. P. Blok, E. Jans, P. H. M. Keizer, L. Lapikás, E. N. M. Quint, G. van der Steenhoven, and P. K. A. de Witt Huberts, Nucl. Phys. A **490**, 507 (1988).
59 W. H. Dickhoff, and C. Barbieri, Prog. Particle Nucl. Phys. **52**, 377 (2004).
60 V. R. Pandharipande, I. Sick, and P. K. A. W. Huberts, Rev. Mod. Phys. **69**, 981 (1997).
61 J. G. Cramer, and R. M. DeVries, Phys. Rev. C **22**, 91 (1980).
62 V. Raghunatha Rao, M. Sudarshan, A. Sarma, R. Singh, S. R. Banerjee, and S. N. Chintalapudi, Nuov Cim A **107**, 1441 (1994).
63 X. F. Zhang, and D. Y. Pang, Chin. Phys. Lett. **31**, 052401 (2014).
64 G. J. Kramer, H. P. Blok, and L. Lapikás, Nucl. Phys. A **679**, 267 (2001).